CONF-830942--22

CONF-830942--22

DE84 000725

LOW-CYCLE FATIGUE BEHAVIOR OF OXYGEN-FREE HIGH-CONDUCTIVITY COPPER AT 300°C IN HIGH VACUUM*

K. C. Liu and C. M. Loring, Jr.

Oak Ridge National Laboratory, Metals and Ceramics Division, P.O. Box X, and Y-12 Plant, Fusion Energy Division, P.O. Box Y, Oak Ridge, Tennessee 37830

In-vacuum fatigue tests were performed on commercially-pure OFHC copper and 35% Au–65% Cu brazing filler metal at 300°C. Excessive recrystallization due to exposure in the 1025°C brazing temperature cycle was detrimental to the fatigue life of the base metal; cold work was beneficial to the fatigue resistance. Triple-point cracking and grain boundary sliding were the prevailing modes of fatigue failure observed in the full-size specimens. However, a mixed morphology of ductile and cleavage-like fracture was observed on the fracture surface of the subsize specimen in which the grain structure appeared to have undergone a change because of the presence of surface cold work. The braze has superior fatigue resistance, but to exploit the maximum strength, the brazed joint must be devoid of defects such as cavities and cracks.

1. INTRODUCTION

Oxygen-free high-conductivity (OFHC) copper will be a major construction material for use in electrical components of fusion power reactor systems. Some large components, such as gyrotron tube collectors, must be fabricated in sections and joined together by brazing. Since gyrotrons are pulse operated, thermal fatigue is a prime concern. Analyses indicate that the maximum internal surface temperature of the gyrotron collector will be approximately 300°C and the resultant peak thermal strain will be approximately 0.3%.[1]

Fatigue data for OFHC copper are scarce, especially data taken in a high vacuum environment. Although limited results of in-air tests[2,3] are available, little or no data can be found in the strain range of our interest. The objective of this experiment is to generate base-line information on the fatigue properties of both base metal and braze to help determine the service life of gyrotron collectors.

2. MATERIAL AND SPECIMEN

Type 101, class 2, OFHC copper was used. It was furnished in the form of two halved shells cut from a forged tubing (16.5-cm OD × 12.7-cm ID × 20-cm length) by Varian Associates. The tubing was cut from the stock used in the construction of gyrotron collectors. One shell contained a girth braze at the mid-length. The brazing filler metal is 35% Au–65% Cu. The brazing was done in hydrogen environment; the brazing cycle was 30 min soak at 980°C followed by 2 min hold at 1025°C. To obtain the same microstructure, the unbrazed shell was subjected to the same temperature cycle also. Fatigue specimens were prepared in two sizes, as shown in Fig. 1. The button-head full-size specimen has a 6-mm gage diameter and 13-mm diameter shanks as recommended by ASTM for use in fatigue testing. Brazed specimens were made with the braze offset 1.5 mm from the center where the diametral strain was measured and used for test control. The subsize specimens

*Research sponsored by the Office of Fusion Energy, U.S. Department of Energy under contract W-7405-eng-26 with the Union Carbide Corporation.

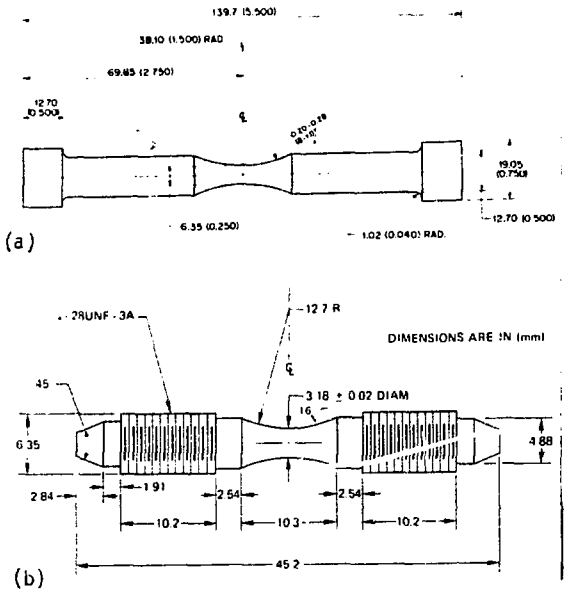

FIGURE 1
(a) ASTM recommended hourglass fatigue specimen with bottom-heads. (b) Subsize fatigue specimen with threaded ends

have a 3-mm gage diameter with other dimensions in the gage section scaled down accordingly. The high rejection rate of flaw-ridden brazed specimens and the consequential depletion of the brazed stock prompted the use of the subsize specimens. Although not shown in Fig. 1, a standard ASTM specimen was machined with a uniform gage section 6 mm in diameter. This specimen was used to generate information for comparison with test results obtained from the hourglass specimens. Post-machining heat treatment was not performed to avoid additional recrystallization. Therefore, special care was exercised to minimize the surface cold-work resulting from the machining. Examinations of micrographs show that the depth of the surface cold work has successfully been limited to about 50 μm or less.

3. FATIGUE TESTING

Tests were performed on a servo-hydraulic closed loop controlled testing system equipped with an ultrahigh vacuum system pumped by a cryopump capable of pressures below 10^{-6} to 10^{-4} Pa. Experimental details are reported in a paper[4] also presented in this meeting.

4. RESULTS

Generally, annealed OFHC copper exhibits pronounced cyclic hardening followed by a period of stable stress strain behavior until failure occurs, as illustrated by curve "A" in Fig. 2. The cyclic stress-strain responses were quite different for the recrystallized OFHC copper used in this experiment as illustrated in Fig. 2. The reason for the uncharacteristic behavior is not known. However, the monotonic hardening feature was demonstrated by specimen SU1, which is a uniform gage specimen, the anomaly was possibly due to the difference in specimen geometry as well as the method of strain measurement. The effect of specimen geometry becomes more pronounced as the cyclic strain range increases. Having been cycled

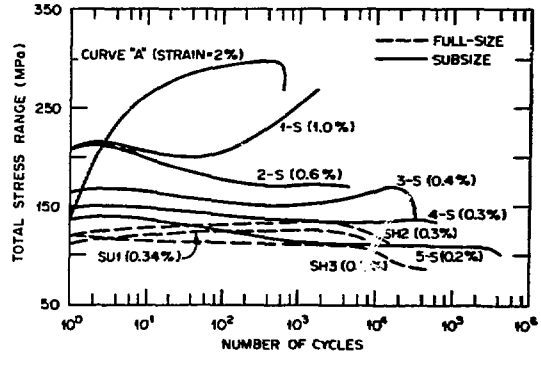

FIGURE 2
Stress response with cycles for OFHC copper tested at various strain

initially at a stress level in excess of the stable stress-strain state, the hourglass specimens should produce reliable fatigue data that are at least equal to or more conservative than those of the uniform gage specimens.

The results of fatigue tests are summarized in Table 1 and plotted on a $\Delta\varepsilon_t$ versus N_f diagram in Fig. 3. Three fatigue curves as shown in Fig. 3 were determined using the following power law equation:

$$\Delta\varepsilon_t = AN_f^{-\alpha} + BN_f^{-\beta} ,$$

where

$\Delta\varepsilon_t$ = total strain range in %, and

N_f = number of cycles to failure.

The values of material constants (A, B, α, and β) are given in Table 2. The upper most curve (curve a) represents the average fatigue behavior of the subsize specimens. The fitting is accomplished using the least square method, excluding the data of specimen B-2, which failed prematurely at the cavities embedded in the braze. The middle curve (curve b) and bottom curve (curve c) are fit visually to approximate the fatigue behavior of the full-size unbrazed

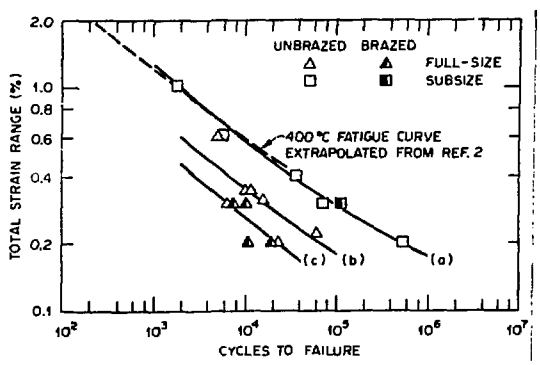

FIGURE 3
Total strain range ($\Delta\varepsilon_t$) as a function of cycles to failure (N_f) for OFHC copper tested at 300°C in vacuum

TABLE 1
Results of in-vacuum fatigue tests on OFHC copper at 300°C

Specimen	Total strain range (%)	Total stress range (MPa)	Crack initiation,[a] N_i	Cycles to failure, N_f
		Subsize fatigue specimens		
1-S	1.0	211	1,250	1,791
2-S	0.6	171	4,200	5,778
3-S	0.4	158	16,500	35,447
4-S	0.3	133	42,000	70,915
5-S	0.2	109	316,000	527,000
B-1	0.3	129	31,000	109,000
B-2	0.2			74,759[b]
		Standard ASTM fatigue specimens		
SH1	0.375	135	6,000	11,070
SH2	0.314	136	5,800	15,494
SH3	0.2	110	18,000	60,916
SH4[c]	0.6	203	1,160	5,141
SH5[d]	0.3	124	4,000	6,543
SH6	0.2	110	18,000	22,479
SU1	0.344	129	7,550	9,879
BH1	0.3	147	8,400	9,910
BH3	0.2	112	10,380	10,690
BH4	0.3	120	4,360	7,168
BH6	0.2	110	18,000	18,757

[a]Crack initiation is determined approximately at the onset of rapid reduction in stress range.

[b]Premature fracture at defective braze joint.

[c]Test section cold worked by unknown amount of torsion.

[d]Ruptured by power outage.

TABLE 2
Material constants for fatigue curve equations
α = 0.097 and β = 0.437

Coefficient	Curve				
	a	b	c	d	e
A	0.48	0.29	0.19	0.45	0.16
B	21.03	12.88	10.21	15.96	10.02

and brazed specimens, respectively. Note that extrapolations of the data outside the test range are not warranted.

The relationship between $\Delta\varepsilon_t$ and N_i (cycles to crack initiation) is depicted in Fig. 4. Because the N_i data show little or no appreciable distinction between unbrazed and brazed specimens, a single fatigue curve (curve e) will suffice. To facilitate comparisons, all three of the N_f curves are also plotted in Fig. 4. Curve d, representing the N_i data of the subsize specimens, falls substantially below curve a by a factor of about two. In contrast, the life after the onset of the crack initiation is very short for the brazed specimens.

5. DISCUSSION

The grain size of microstructure is known to be an important factor that can influence the cyclic fatigue life of metals. Previous fatigue tests show that small grain size is beneficial to the fatigue resistance. The optimum grain size is not known for OFHC copper. However, it should be in the range of 30 to 50 μm, which is an optimum value for most stainless steels, also fcc materials.

Examinations of micrographs shown in Figs. 5 and 6 indicate that the average grain size is about 250 μm for the present specimens. Larger grains in excess of 500 to 700 μm are observed in some of the specimens. The excessive recrystallization, which is an inadvertent consequence of exposure to the high-temperature brazing cycle, undoubtedly reduced the fatigue resistance. Although a direct comparison can not be made because of the difference in test temperature, Fig. 3 shows that the fatigue performance of the full-size specimen is significantly inferior compared with that

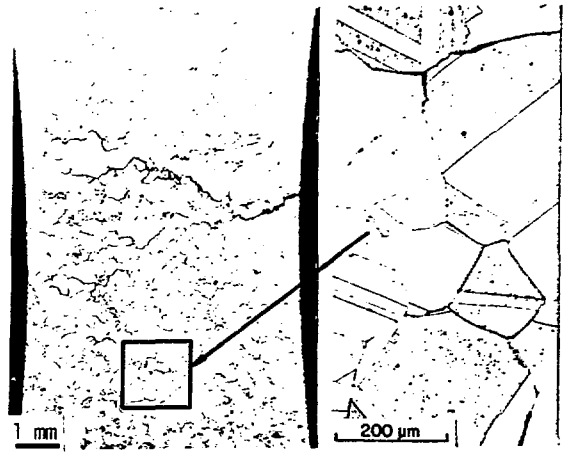

FIGURE 5
Photomicrographs of fatigue-failed full-size fatigue specimen (specimen SH5)

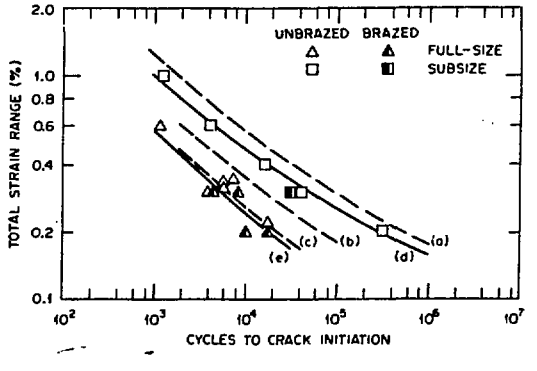

FIGURE 4
Total strain range ($\Delta\varepsilon_t$)as a function of cycles to crack initiation (N_i)

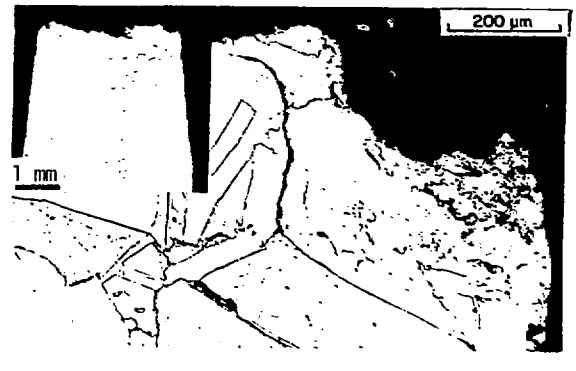

FIGURE 6
Photomicrographs of fatigue-failed fatigue specimen (specimen 4-S)

reported in ref 2, where the grain size of the OFHC copper was reported to be about 90 μm.

The fracture surfaces were studied by scanning electron microscopy (SEM) to help determine the fatigue failure mechanism. For the subsize specimens (Fig. 7), the surfaces showed almost exclusively ductile rupture, except in the center region where the fracture surface showed a mixed morphology of ductile and transgranular cleavage-like rupture. In contrast, intergranular cracking was the prevailing mode of fatigue failure for the full-size specimens as shown in Fig. 8. However, the mode of the failure around the periphery of the fracture surface showed a ductile feature similar to that observed in the fractured subsize specimens.

The micrograph for specimen SH5 (Fig. 5) revealed that this specimen was damaged extensively along the grain boundaries resulting in a network of visible cracks which extended deeply in the shoulder section. This observation suggests that the fatigue failure was most likely initiated by triple-point cracking which in turn was associated with grain boundary sliding. Contrasting the above observation, the grain structure of the subsize specimen appears to have undergone a change of morphology during the cycling. The micrograph in Fig. 6 shows that there was substantial cold working in the bulk material. As a result, the grain boundaries in the fracture region were deformed irregularly with the formation of many small subgrains. The reason for the grain structure in the subsize specimen undergoing the change is not known. For the subsize specimen with fewer grains across the diameter, it is possible that grain boundary migration can take place more readily during cycling, whereas the grains in the large specimen are more restricted to rotate. Hence, the internal balance of the stress and strain between the grains results in grain boundary sliding. Furthermore, because the grain boundary sliding constitutes most of the strain imposed on the large specimen, the internal stresses required to generate the same strain will be higher for the subsize specimens with no grain boundary sliding.

Bucking the general data trend of large specimens, specimen SH4 exhibited the best performance among its data group. Because this specimen was cold-worked accidentally in torsion during the machining as shown in Fig. 9, we believe that the high fatigue resistance

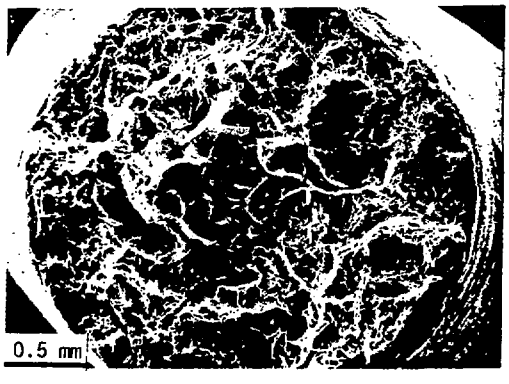

FIGURE 7
Scanning electron micrograph of fracture surface of specimen 4-S

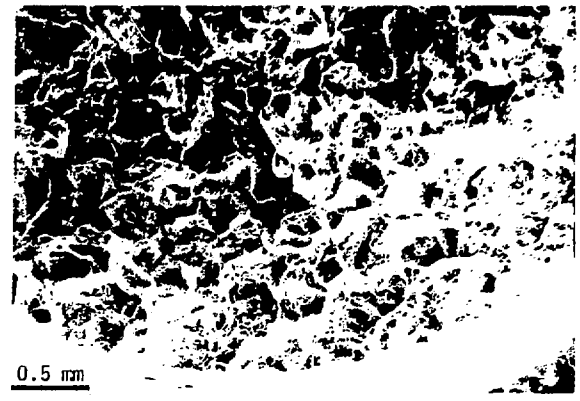

FIGURE 8
Scanning electron micrograph of fracture surface of specimen BH4

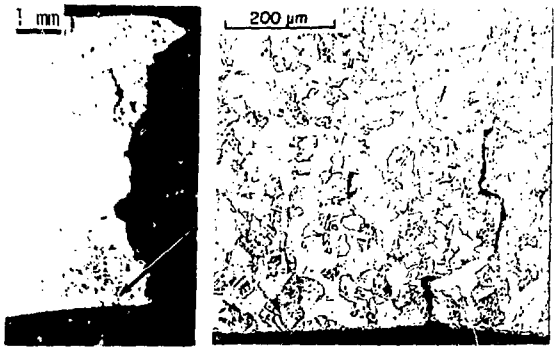

FIGURE 9
Photomicrograph of specimen SH4 cold-worked by torsion

must be attributed to the cold working. However, Fig. 4 shows that the torsional cold working did not appear to enhance its ability to resist the initial cracking.

It is important to note that no tests have failed at the braze unless defects such as cavities were present in the braze. The micrograph in Fig. 10 shows that the total absence of triple-point cracking in the proximity of the braze resulted from the diffusion of gold which apparently enhanced the grain boundary cohesion. However, grain boundary sliding and cracking are still visible in the region away from the influence of the braze. This observation suggests that the increased grain boundary strength in the localized section could introduce additional stresses in the grain structure adjacent to the braze-affected zone. Hence, the brazed specimens exhibit the lowest fatigue performance.

6. CONCLUSIONS

1. Results obtained from in-vacuum fatigue tests showed that this stock had unusually low fatigue resistance compared with available test data. Low grain boundary strength, attributable to excessive recrystallization, accounted for the low fatigue performance.

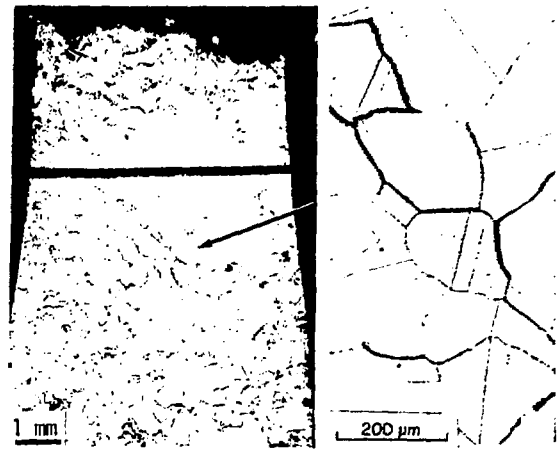

FIGURE 10
Photomicrographs of fatigue-failed brazed specimen (specimen BH4)

2. Cold work was found to be beneficial to the fatigue resistance of the material.

3. The 35% Au–65% Cu braze had not only superior fatigue resistance but also enhanced the grain boundary strength of the base metal in the proximity to the braze joint.

8. REFERENCES

1. J.A. Clinard, private communication.

2. G. Wigmore and G.C. Smith, "The Low-Cycle Fatigue Behavior of Copper at Elevated Temperatures," Met. Sci. J., 5 (1971) 58.

3. H. Abdel-Raouf, A. Plumtree, and T.H. Topper, "Temperature and Strain Rate Dependence of Dependence of Cyclic Deformation Response and Damage Accumulation in OFHC Copper and 304 Stainless Steel," Met. Trans., 5 (1974) 267.

4. M.L. Grossbeck and K.C. Liu, "Fatigue Performance of HFIR-Irradiated NIMONIC PE-16 at 430°C," Third Topical Meeting on Fusion Reactor Materials, Albuquerque, N.M., Sept. 19–22, 1983.